Identification of noise sources using a time domain beamforming on pneumatic, gas and electric nail guns

Thomas Padois[a)], Marc-André Gaudreau[b)], Pierre Marcotte[c)] and Frédéric Laville[a)]

(Received: 11 June 2018; Revised: 22 January 2019; Accepted: 23 January 2019)

In the construction industry, many workers are exposed daily to harmful levels of impulsive noise from nail guns. Therefore, a better knowledge of the noise generated by these tools is required in order to propose noise reduction solutions. The objective of this work is to propose an approach for source identification using a microphone array together with a source identification algorithm based on recent development in the generalized cross-correlation technique. In addition to the pneumatic nail gun, for which sources have been partially identified in the literature, the proposed approach is applied to two other types of nail guns, an electric and a gas powered one. First, the standardized acoustic power spectrum of these three nail guns is measured for global comparison purposes and result in a ranking of the three nail guns. Second, the generalized cross-correlation technique applied to nail gun noise source identification is presented. Third, acoustic maps for successive small time segments are presented, providing a fine identification of noise sources for the three nail guns and an explanation of the observed sound power level ranking.

Primary subject classification: 74.6; Secondary subject classification: 11

1 INTRODUCTION

Nail guns are common power tools used in the construction industry. Such tools can be dangerous as they may cause injury or death[1]. In addition, they expose workers to high levels of impulsive noise[2] and vibration[3].

From the point of view of noise exposure, noise emission values of several nail guns have been used in order to estimate the hearing loss risk associated with these tools[2]. The equivalent A weighted single-event sound pressure level over 1 s for a framing nail gun in real use/simulated measurements ranges from 89 to 100 dBA[2,4]. Such levels could make the noise of nail guns a significant contributor to the risk of hearing loss when the total number of events per workday is high. For example, some workers in the wood pallet industry will drive 12,000 nails in 8 h so that their daily personal exposure will range between 85 and 96 dBA.

Previous studies on nail gun noise have focused on pneumatic type of nail guns. In 2003, Hicks et al.[5] presented the use of time domain observations of the sound pressure signal from which they identified four pressure peaks that could be associated to four events, two of them being identified as major noise sources: the initial impact of the piston hitting the stopper and the air exiting the exhaust. New bumper materials inside the nail gun and different mufflers were then proposed in order to reduce the noise emitted by the nail gun. In 2016, Nili Ahmadabadi et al.[6] also presented time domain observations and their work led to a more detailed identification of the noise generation mechanisms with the use of additional signals from a high speed camera, accelerometers on the nail gun housing and two pressure transducers (one inside the chamber that moves the piston and another one in the return chamber). In 2015, Jayakumara et al.[7] presented an investigation of the noise generated by a pneumatic nail gun also using a sound pressure time history analysis, to which they added sound source images using a microphone array. The time history was divided into four parts, which consist in the compressed air flow through the inlet port, the piston strike, the nail impact and the air exhaust. They also used noise absorbing foam on the outside of the nail gun body or mufflers onto the exhaust in order to reduce the overall noise level.

Although that study added acoustic imaging technique to the other ones, many additional information would be necessary in order to reliably reproduce their noise source identification technique. First, the time window of the acoustic signal was set to 2.82 ms, but the lengths of the time segments shown in the figure were different. Then, the microphone array geometry, the source-array distance and the post-processing technique were not provided. Finally, the colorbar and dynamic range were not shown in the figure, which prevents a full analysis of the acoustic maps.

[a)] Department of Mechanical Engineering, École de Technologie Supérieure, Montréal, CANADA; email: Thomas.padois@etsmtl.ca.
[b)] Department of Mechanical Engineering, Univsersité du Québec à Trois-Rivières, Drummondville, CANADA.
[c)] Institut de Recherche Robert-Sauvé en Santé et en Sécurité du Travail, Montréal, CANADA.

The objective of this study is to propose a detailed approach for source identification on nail guns using a microphone array together with a source identification algorithm based on recent development in the field. Several source localization algorithms exist in the literature. The most standard technique in the far-field is beamforming, which can be used in the frequency[8,9] or time domain[10,11]. In the frequency domain, the microphone signals are divided into time segments, then the cross spectral matrix is computed for each segment and finally averaged in order to remove background noise. This technique allows for generating acoustic maps for each discrete frequency of the cross spectral matrix. For example, if an acoustic source generates a tonal noise, the cross spectral matrix at this frequency has to be selected to generate the acoustic map. In the case of nail gun noise, the acoustic signal is an impulse that lasts only a few milliseconds. Therefore, an efficient average of the cross spectral matrix is not possible. Moreover, the noise spectrum of the nails guns is generally broadband, making it difficult to select which discrete frequency to analyze. Finally, as the time signal is very short, the frequency resolution of the cross spectral matrix is large. Consequently, for these reasons, a time domain beamforming should be used.

The source identification technique used in this article is based on the generalized cross-correlation (GCC)[12] and can be seen as a broadband beamforming technique. This technique allows for taking very small time segments to perform source identification. More details on this approach and on recent development in the field of beamforming imaging techniques are available in the following references[13–16].

To complete other studies available in the literature that are limited to pneumatic nail gun, alternative technologies consisting of an electric and a gas powered nail guns are also presented in the applications of the proposed approach. First, the acoustic power spectrum of these three nail guns are obtained from standardized acoustic measurements for global comparison purposes. Second, the experimental set-up and calibration procedure are presented. Finally, acoustic maps for successive small time segments are presented and discussed for each of the three nail guns.

2 ACOUSTIC SOUND POWER LEVEL OF THE THREE NAIL GUNS

2.1 Experimental Set-up in a Hemi-anechoic Chamber

The experimental set-up was designed to measure the acoustic power of nail guns according to the standards ISO 3744[17] and EN12549[18]. The measurements took place in the hemi-anechoic chamber of the ÉTS laboratory. A standardized piece of wood (pine) was buried in a sandbox. The nail gun was held by a handle, which was secured onto an aluminum frame (see Fig. 1a). A custom made

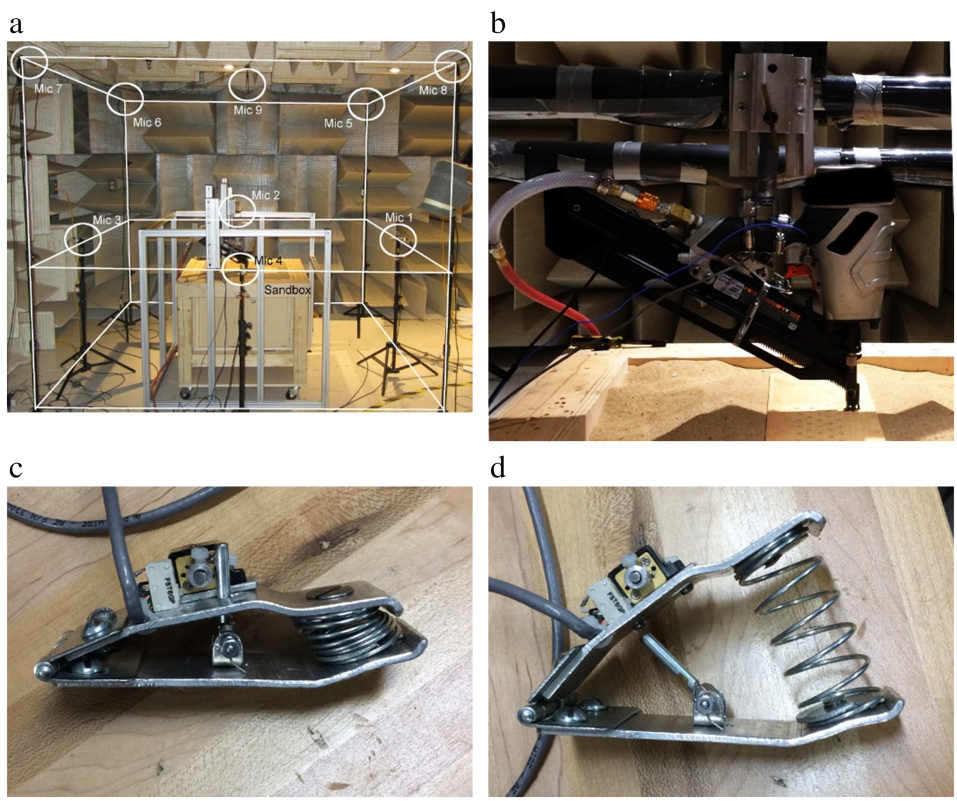

Fig. 1—Pictures of (a) The experimental set-up with the 9 microphones cubic grid and the sandbox, (b) The nail gun, (c) The armed and (d) Fired custom made trigger.

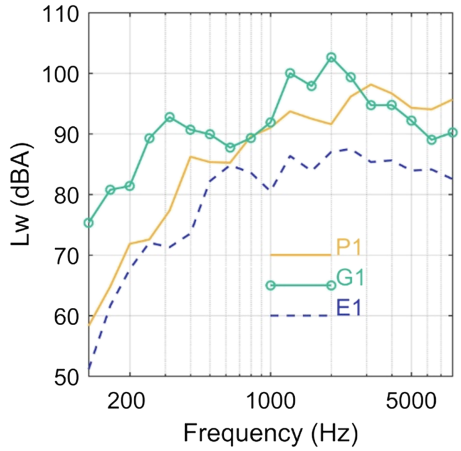

Fig. 2—A-weighted power spectra in third-octave band for the three nail guns (P1: pneumatic, E1: electric and G1: gas).

trigger was developed to remotely operate the nail gun from outside the hemi-anechoic chamber (see Fig. 1b–d), without the presence of a human subject in the hemi-anechoic chamber.

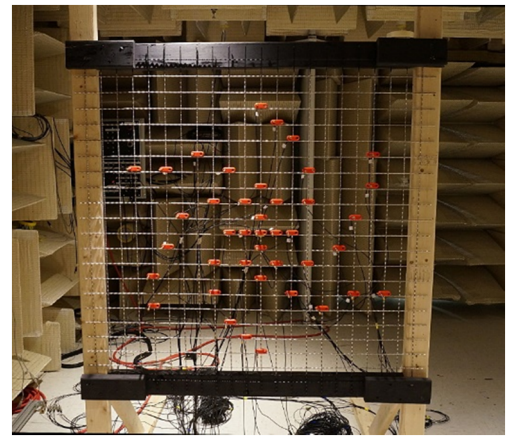

Fig. 3—Picture of the 41 microphones spiral-arm array.

The acoustic signals were recorded by 9 MPA-231 BSWA microphones located in a cubic grid (2 m edge) as described by the standards[17,18] with a microphone in each corner and in each face center (see Fig. 1a). The microphone signals were recorded by a Sound and Vibration Module PXIe 4497 and sampled at 51,200 Hz.

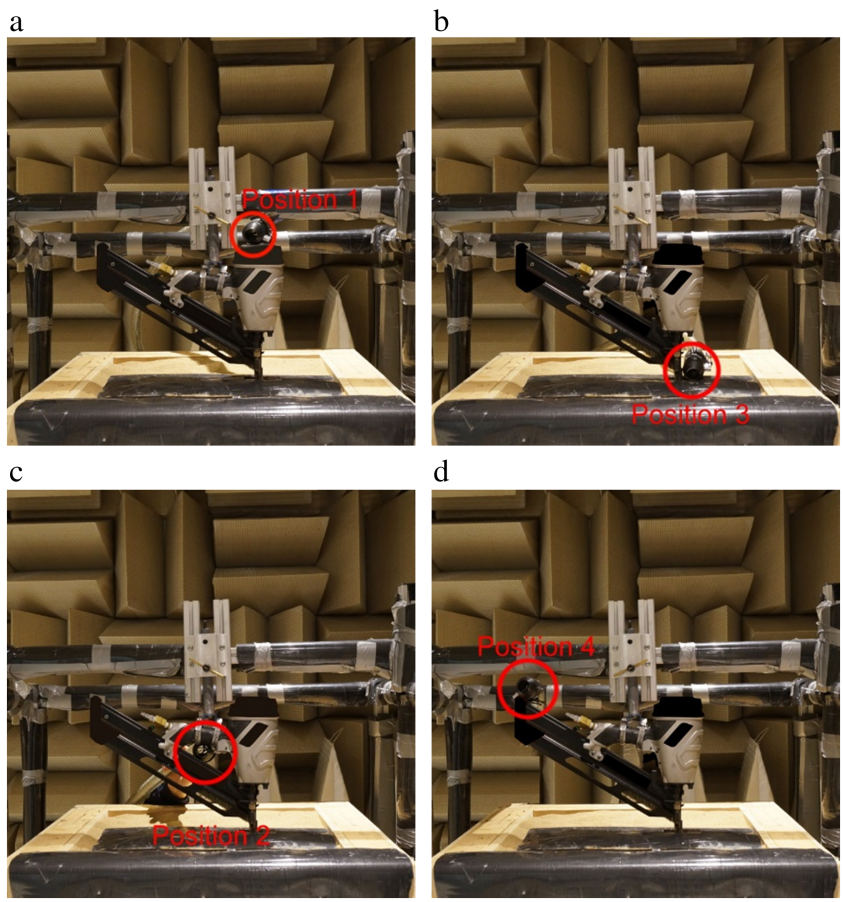

Fig. 4—Pictures of the P1 nail gun with the different position of the volume source: (a) Top, (b) Piece of wood, (c) Trigger and (d) Extremity of the strip.

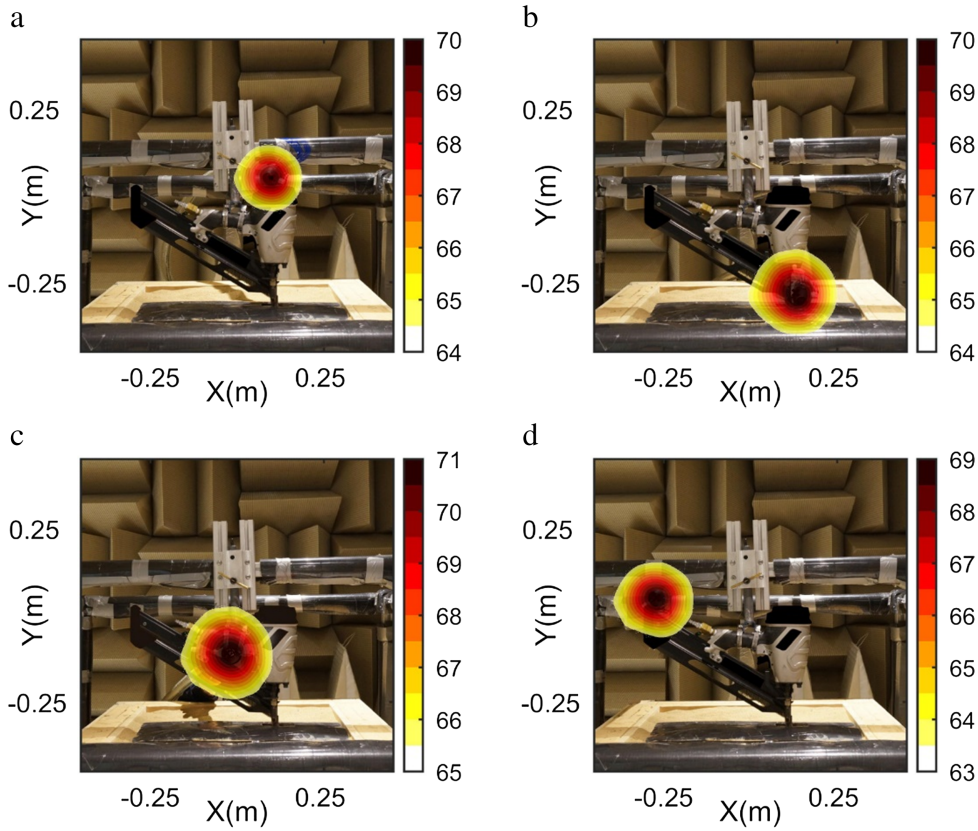

Fig. 5—Acoustic maps of the P1 nail gun in the case of the volume source: (a) Top, (b) Piece of wood, (c) Trigger and (d) Extremity of the strip.

The nail guns are identified as P1, G1 and E1 for respectively the pneumatic, gas and electric nail gun (nail gun brands are deliberately not provided).

2.2 Acoustic Sound Power Spectrum

The microphones simultaneously recorded the impulsive noise generated by the nail guns. Then, the 1 s equivalent single-event A-weighted sound pressure levels, denoted $L^i_{pA,1s}$, were computing using the following:

$$L^i_{pA,1s} = L^i_{pA_{eq}T} + 10\log_{10}\frac{T}{T_0} \qquad (1)$$

where $L^i_{pA_{eq}T}$ is the A-weighted sound pressure level for the microphone i over the measurement interval T (in seconds) and T_0 corresponds to 1 s for the microphone i. Based on the sound pressure level at each microphone position, the acoustic power level L_W has been computed such as:

$$L_W = 10\log_{10}\left(\frac{1}{9}\sum_{i=1}^{9} 10^{\frac{L^i_{pA,1s}}{10}}\right) + 10\log_{10}(S), \qquad (2)$$

where S is the measurement surface (here $S = 20$ m^2).

The A-weighted power spectra, averaged over 10 trials, are shown in Fig. 2. The spectra are presented in one-third octave band in the 100–8000 Hz range. The E1 nail gun presents the lowest sound power level. More so, it is noticeable that the sound power level of this nail gun is the lowest for the full frequency range. The G1 nail gun generates the highest sound power level at low frequency, especially around 300 Hz, where the sound power level is 15 dB larger than the sound power of the P1 nail gun and 20 dB higher than the E1 nail gun. The highest sound power level (103 dBA) is reached around 2000 Hz with the G1 nail gun. Above 3000 Hz, the sound power level generated by the G1 nail gun decreases below the P1 sound power level. This standardized measurement allows for ranking the nail gun, but does not provide any information on the noise sources mechanisms. Therefore, a noise source identification based on the time domain beamforming technique presented in the introduction is presented in the next section.

3 NOISE SOURCE IDENTIFICATION ON NAIL GUNS

3.1 Experimental Set-up in a Hemi-anechoic Chamber

A 41 microphones spiral-arm array with a 1 m aperture was located at 2 m from the nail gun (see Fig. 3). The acoustic signal was measured with Bruel&Kjaer microphones type 4935 and recorded by a 12-Channel input

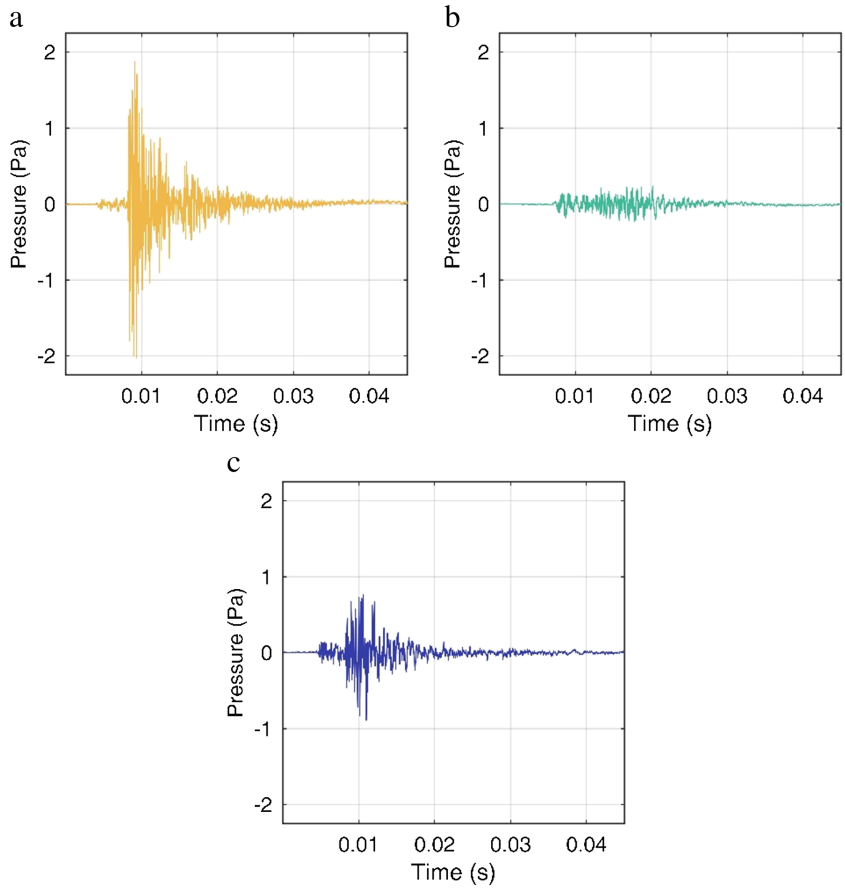

Fig. 6—Acoustic time signals of the custom-made trigger for (a) P1, (b) G1 and (c) E1 nail guns.

module type 3038B at 32,768 Hz sampling rate. The nail gun was remotely controlled outside the hemi-anechoic chamber. A noise barrier (see Fig. 4, in black below the nail gun) was added onto the piece of wood to reduce its noise radiation in order to focus on the nail gun noise only.

3.2 Calibration Procedure for the Camera and the Microphone Array

The technique for the source identification is to superimpose the acoustic map on a picture of the nail gun in order to detect the source positions. However, before generating the acoustic map, it is important to calibrate the picture of the nail gun with respect to the microphone array position. A camera was set in the center of the microphone array in order to take a picture of the nail gun. Then, a mid-frequency acoustic volume source BSWA VSS 210, using white noise, was set close to the nail gun and a picture of the nail gun with the source was taken (Fig. 4). Four positions of the volume source were tested:

- on the top of the nail gun,
- on the piece of wood,
- close to the trigger,
- at the extremity of the nail strip.

When the source position is well detected, the microphone array and the camera are correctly calibrated for performing source identification on the nail gun.

For each case, time segments with 8192 samples were used and were filtered by a 2nd order bandpass Butterworth filter with cut-off frequencies of 1 and 15 kHz. The scan zone, where the source was searched, was a square with 0.5 m sides located 2 m away from the array. The scan zone was sampled with 101 points in each direction, which leads to a total of 10,201 points and a grid spacing of 0.01 m. The acoustic maps provided by the GCC in the case of the P1 nail gun are shown in Fig. 5. For each case, the source is detected at the correct position, which means that the camera and microphone array were correctly calibrated. One can notice that the main lobe size is larger when the source is close to the trigger (Fig. 5c). This fact may be explained by the reflections on the body of the nail gun, which may occur at that position.

These calibration steps have been also performed with the G1 and E1 nail guns. The acoustic maps for G1 and E1 are not shown here, but similar results were obtained.

3.3 Influence of the Custom Made Trigger Noise

Since noise can be generated when the nail gun trigger is activated, the last step before performing source identification

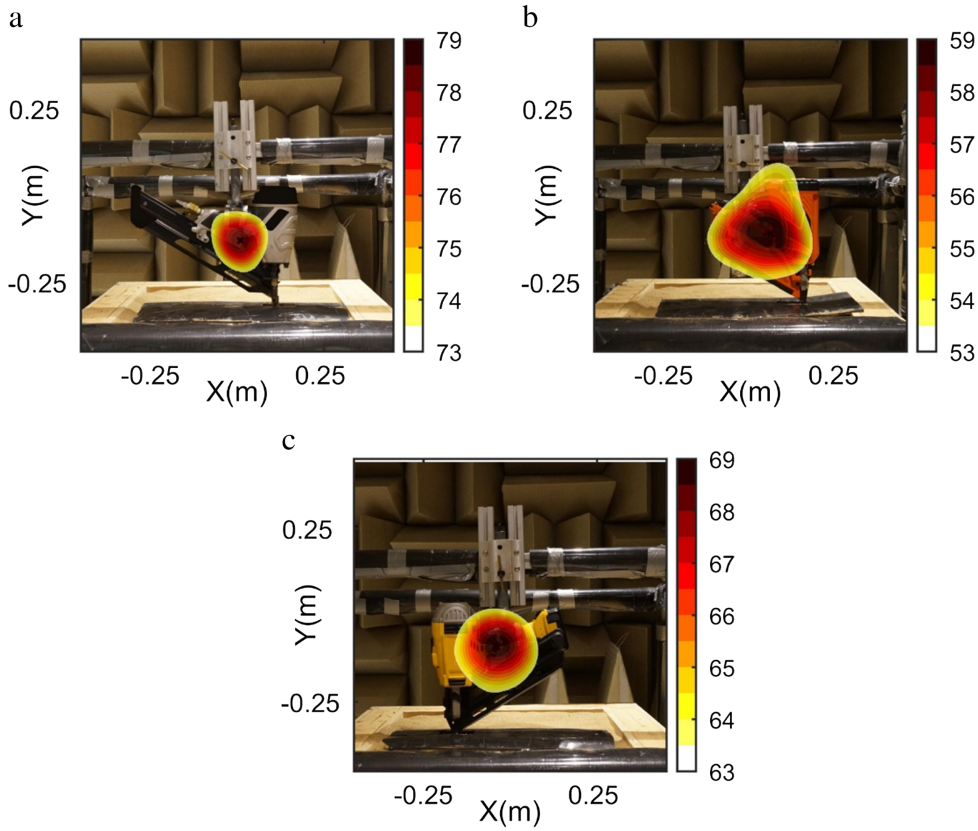

Fig. 7—Acoustic maps of the custom-made trigger for (a) P1, (b) G1 and (c) E1 nail guns.

on the nail guns was to assess the noise contribution of the custom made trigger. This trigger is made with a hinge and two plates connected by a spring (Fig. 1c and d). A notched rod holds the two side of the spring-loaded. When activated, an electric motor with an eccentric shaft pushes the rod that releases the spring energy to trigger the nail gun.

The acoustic signal recorded by the microphone at the center of the array is presented in Fig. 6 for each nail gun. With the P1 nail gun, the custom-made trigger noise is an impulse with an exponential decay. The peak amplitude is almost 2 Pa and the time length is around 20 ms. With the G1 and E1 nail guns, the noise generated is different. The lowest amplitude is provided with the G1 nail gun which is around 0.2 Pa. The G1 nail gun has a small opening between the handle and the nail strip magazine; therefore, the custom-made trigger cannot be fully opened, resulting in a lower sound level. With the E1 nail gun, the amplitude is around 0.8 Pa, with a similar decay than with the P1 nail gun.

Now, the acoustic time signals described in Fig. 6 are used with the GCC to detect the source position of the custom-made trigger. The obtained acoustic maps are presented in Fig. 7. For each case, the position of the custom-made trigger is correctly detected. As expected, the highest sound level is provided by the P1 nail gun. With the G1 nail gun, the main lobe size is larger than that of the two other nail guns. Due to the low sound level of the custom-made trigger, the sound radiation of the handle can be observed and the lobe is extended. With the E1 nail gun, the main lobe size is larger than the main lobe size of the P1 nail gun, but smaller than the main lobe size of the G1 nail gun. To conclude, the custom-made trigger noise is a short impulse with a relatively low sound pressure level.

3.4 Acoustic Signals of the Nail Guns

As the camera and microphone array are calibrated and the custom made trigger noise characterized, the source identification can be performed on the noise generated by the nail guns. The acoustic time signal recorded by the microphone at the center of the array is shown in Fig. 8 for each nail gun. In order to get the same time length, 2048 points are kept before and 4096 after the peak amplitude (corresponding to 0.1875 s). The pressure range is the same for each figure in order to properly compare the nail gun signals. The sound pressure levels are also plotted in Fig. 8, using the root mean square of the time signal with 128 points and no overlap.

The time signals generated by the three nail guns are impulsive; however, they exhibit different features. The P1

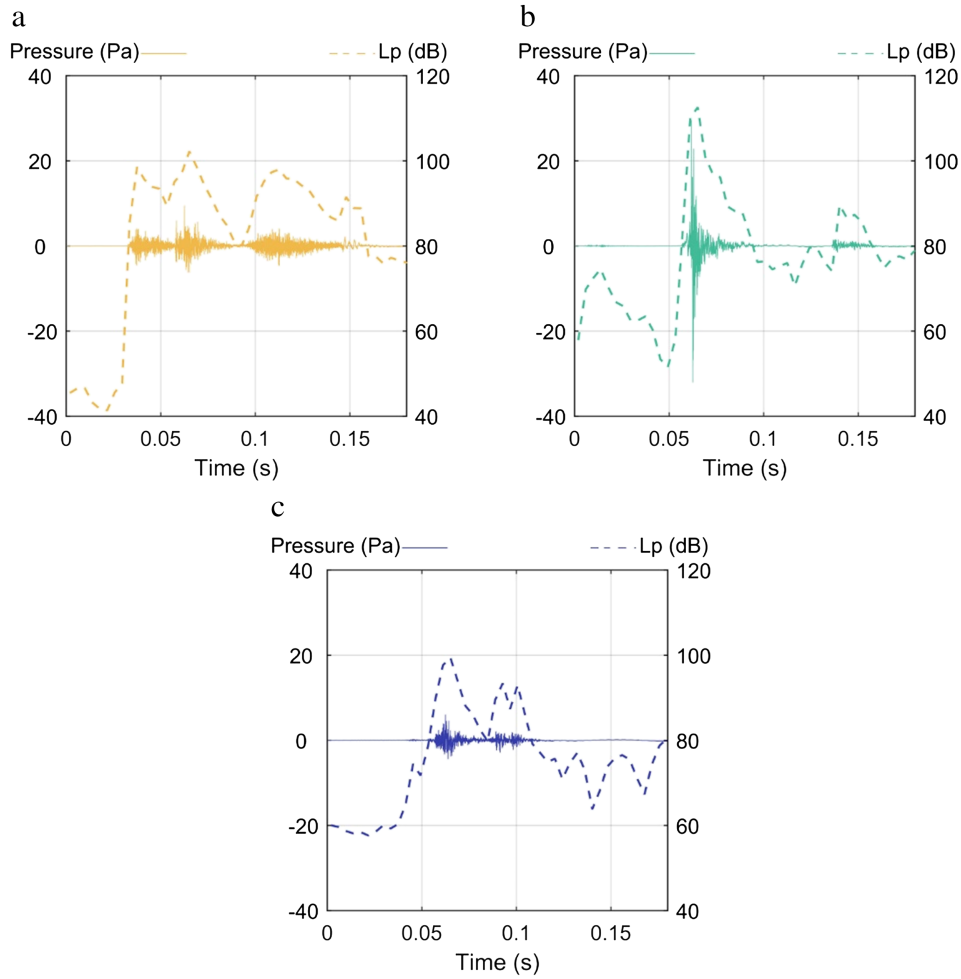

Fig. 8—Acoustic time signals of the (a) P1, (b) G1 and (c) E1 nail guns.

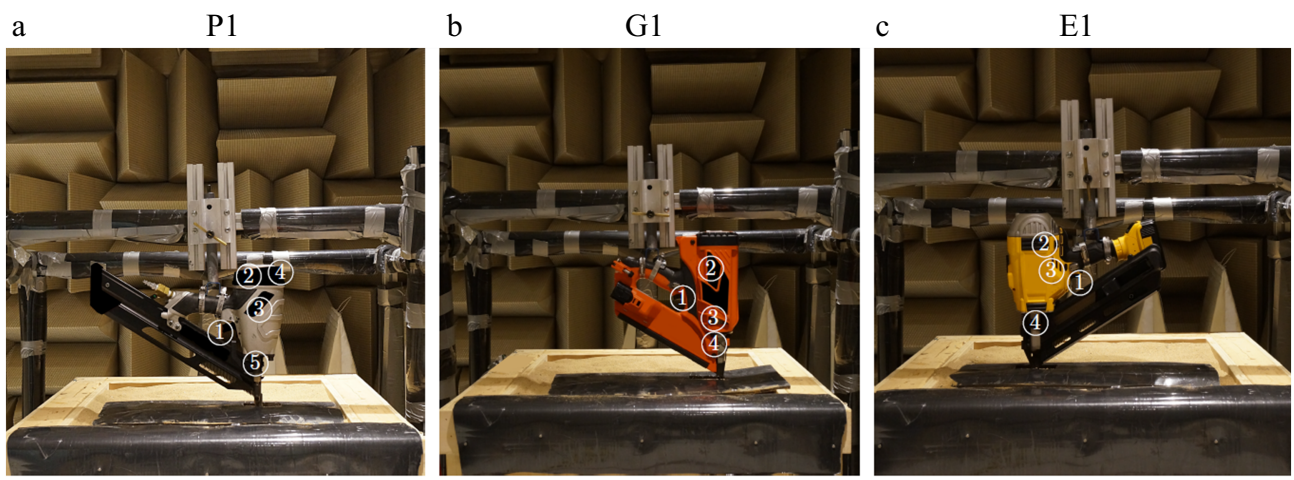

Fig. 9—Key parts of the nail guns.

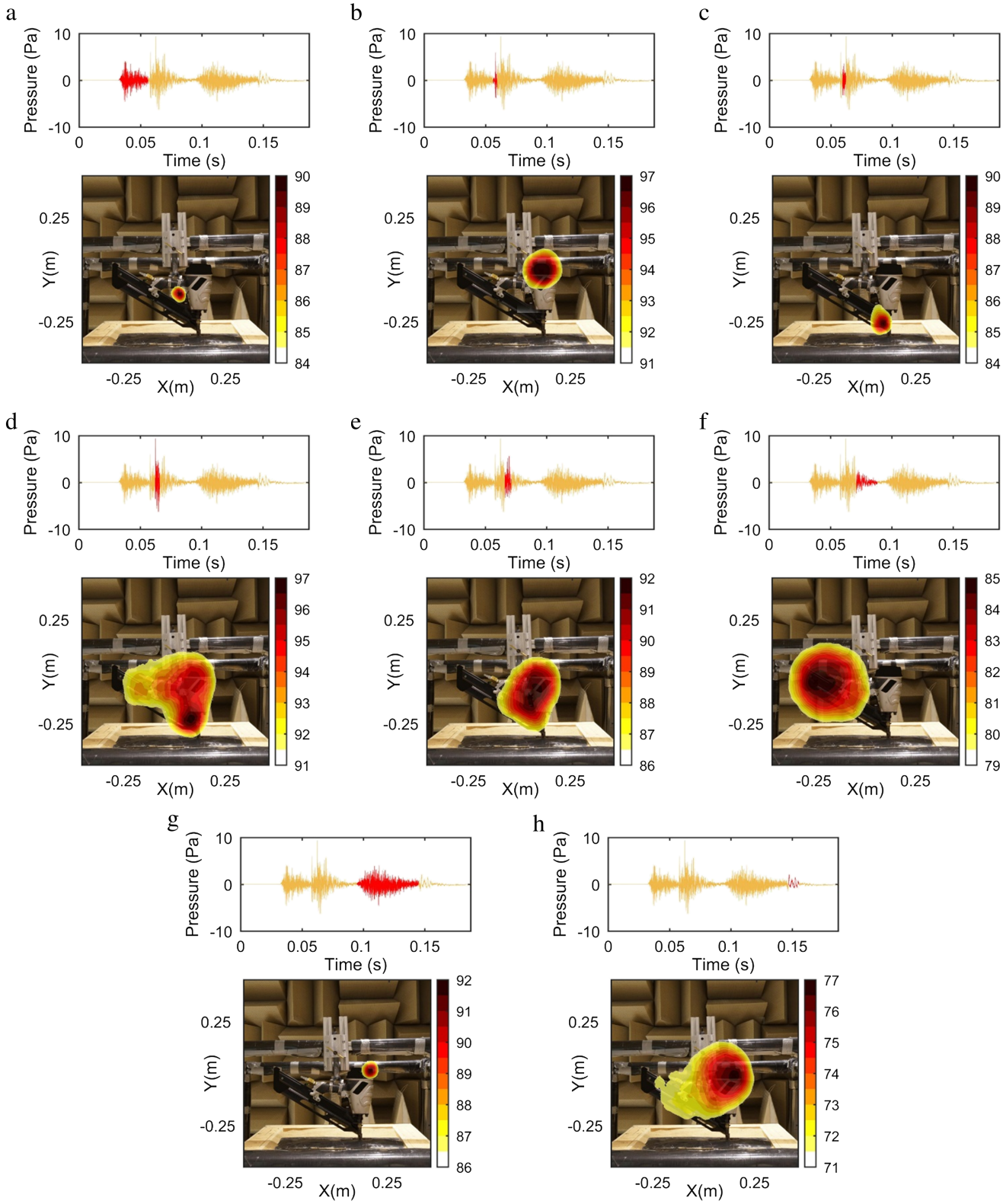

Fig. 10—Acoustic maps of the P1 nail gun. In yellow is the acoustic signal recorded by a microphone. In red is the signal used with the source identification technique.

nail gun generates an impulse of 120 ms length. Three time segments are clearly distinct, with almost the same sound level for each segment. The G1 nail gun generates a very brief impulse of 30 ms length and present the highest sound level. Another time segment is also present 50 ms after the peak amplitude with a lower sound level. Finally, the E1 nail gun produces three segments, two with low levels and one with a higher sound level. Based on these time

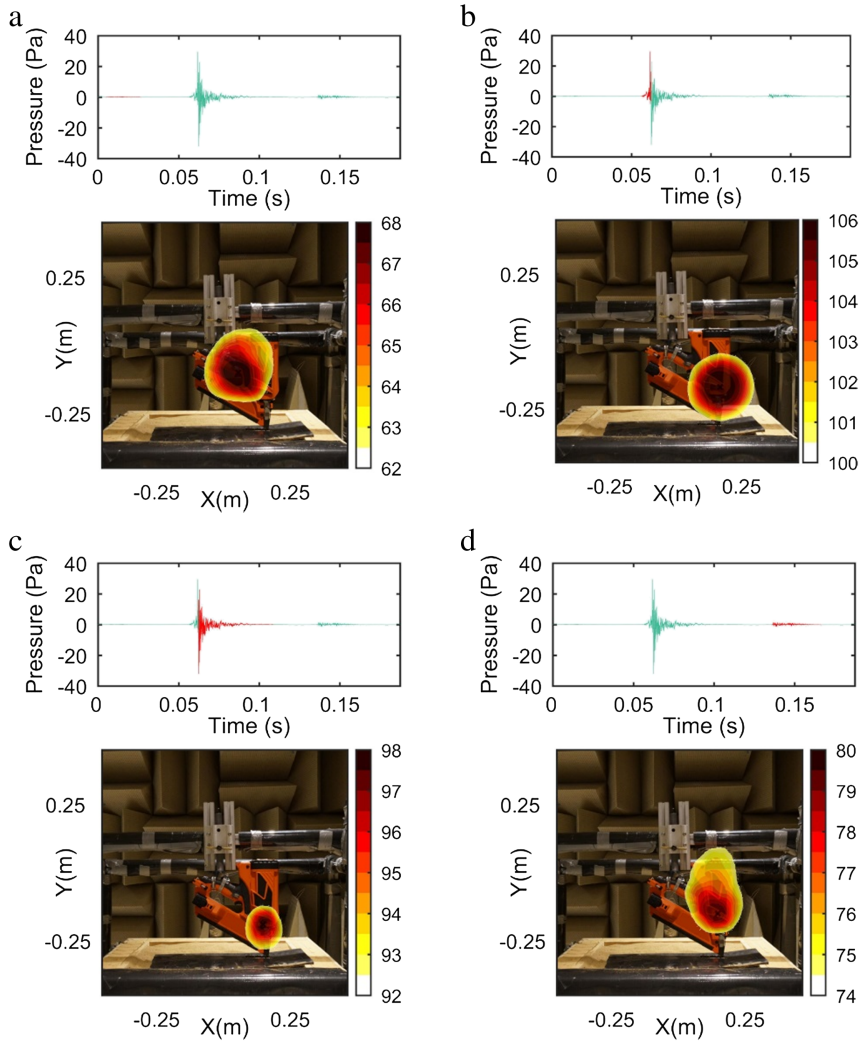

Fig. 11—Acoustic maps of the G1 nail gun. In green is the acoustic signal recorded by a microphone. In red is the signal used with the source identification technique.

segments, it is impossible to define which parts of the nail guns generate noise; thus, a source identification technique is necessary to identify the parts of the nail guns that generate the different time segments. The key parts of the nail guns are presented in Fig. 9 to facilitate the analysis of the acoustic map.

3.5 Pneumatic Nail Guns (P1)

In order to perform the noise source identification, the microphone signals are divided into small time segments, which are used as inputs to the GCC. The geometric mean of the GCC, proposed by Padois et al.[13], is used in the following in order to improve the quality of the acoustic maps.

The time signal, of 120 ms duration, is divided into 8 time segments, allowing the generation of 8 acoustic maps. First, when the custom-made trigger actuates the trigger valve, air is released above the trigger valve. These two events can be identified in Fig. 10a, where a main spot is located at the trigger position. It should be noticed that the GCC associated to the geometric mean clearly improves the acoustic map resolution as compared to Fig. 7a. When the air is released, the pressure is released above the head valve plunger, it suddenly moves up and impact the nail gun body while ejecting some air through the exhaust port (first noise source) and the pressurized air is rushing in the chamber above the piston (second noise source). Both sources are located at the top of the nail gun, as shown in Fig. 10b. In Fig. 10c, the piston is driven down until the impact of the nail driver blade and nail penetrating the wood (the wood radiation is minimized due to the worked piece being buried in sand and covered by a noise barrier material) and the simultaneous impact of the piston with the rubber end stops. After the impact between the piston and the end stops, noise is radiated by the nail gun body (Fig. 10d–f). Then, the piston goes up and the main noise source, as shown in Fig. 10g, is the air being exhausted. When the

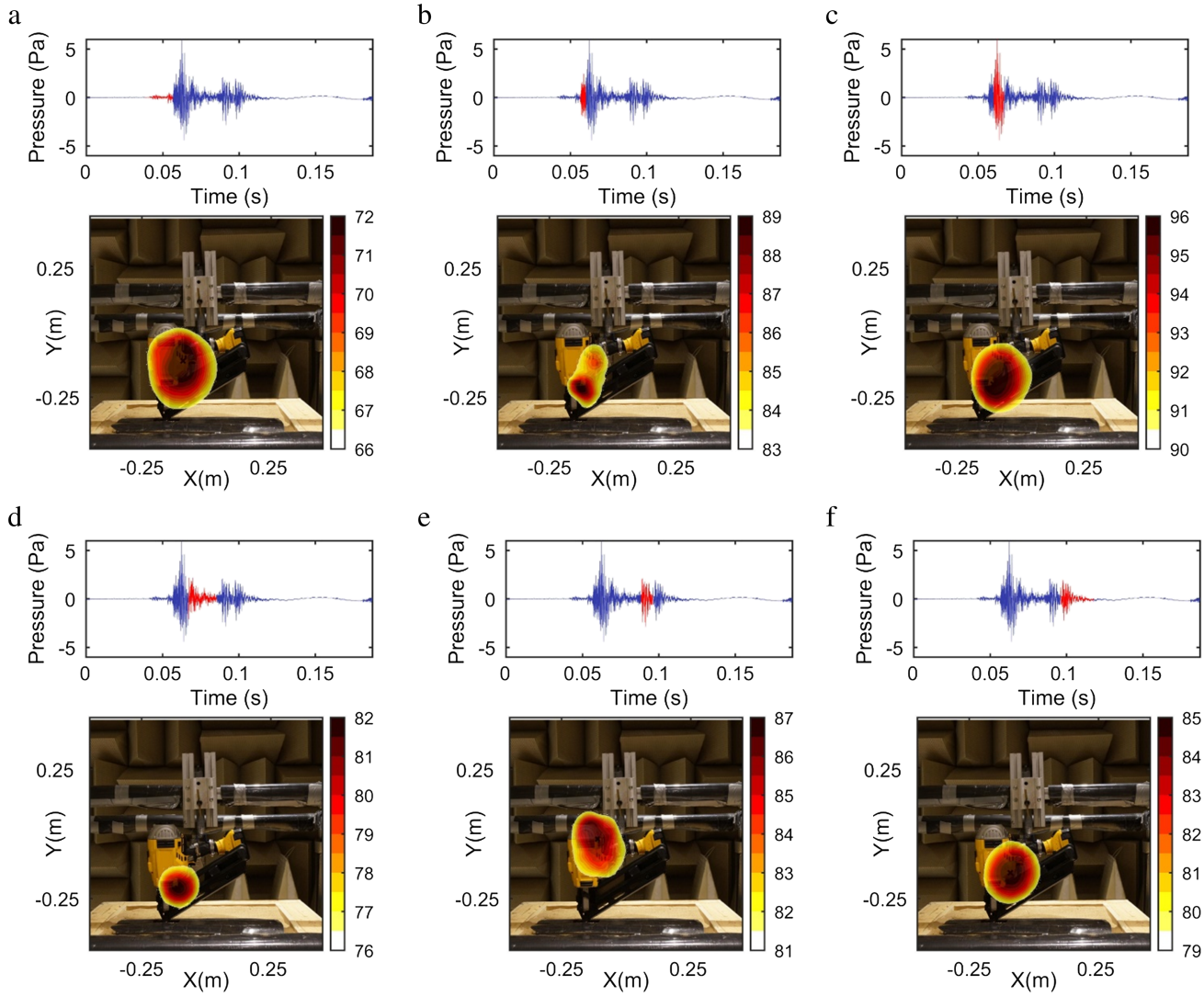

Fig. 12—Acoustic maps of the E1 nail gun. In blue is the acoustic signal recorded by a microphone. In red is the signal used with the source identification technique.

piston hits the high position end stops (initial position), noise is again radiated by the nail gun body, as shown in Fig. 10h. Based on the trend of the sound level shown in Fig. 10a, three events produce the highest sound level. With the noise source identification technique used in this study, these events can be clearly associated to the trigger valve, the piston hitting on the rubber stops and the air exhaust, which is in agreement with a previous study[7].

3.6 Gas Nail Guns (G1)

The impulsive signal provided by the G1 nail gun is the shortest; therefore, it is more difficult to divide it into several parts. The first time segment identified is the custom made trigger noise, few milliseconds before the impact (Fig. 11a). As compared to the total nail gun noise, this contribution is considered as non-significant. In order to fire a nail, the G1 nail gun needs to be pushed down against the surface before pulling down the trigger. This action closes the exhaust and quickly fills the combustion chamber with gas that is mixed with air by a fan. Then, a spark plug ignites the gas causing an explosion (Fig. 1b), which is a major source of excitation to the body of the nail gun, as seen in Fig. 11. In Fig. 11c, the same noise generation mechanisms as in the case of the pneumatic nail gun occur; the impact due to the nail driver blade penetrating the wood produces little radiation and the piston hitting the rubber end stops causes a strong radiation of the nail gun body. Figure 11d shows the exhaust noise which is radiated when the nail gun is lifted from the nailed surface, the exhaust opens and a fan blows the burned gas out.

3.7 Electric Nail Guns (E1)

The time signal provided by the E1 nail gun is composed of three main events with different sound levels.

As for the G1 nail gun, the E1 nail gun has to be pushed against the surface to be nailed before it can fire. This procedure activates the rotation of a flywheel at high speed. When the trigger is depressed, an electromagnetic clutch squeezes the blade (mobile part that hits the nail) onto the flywheel. The blade is sent down, at the tangent speed of the flywheel, to ram the nail. The blade is spring loaded to return to its original position when the nail has been ejected. Figure 12a shows the noise generated by the rotation of the motor and the flywheel before the impact. In Fig. 12b, the blade is engaged with the flywheel and hit the nail (bottom source) while some noise is also escaping from an opening where the motor-flywheel is located (second source above the first one slightly to the right). In Fig. 12c and d, the same noise generation mechanisms, as in the case of the pneumatic and the gas nail guns, occur; the impact due to the nail driver penetrating the wood produces little radiation and the driver hitting the rubber end stops causes a strong radiation of the nail gun body. In this case, the radiation of the body is not as important as for the other two nail guns since the shell of the E1 nail gun is all plastic made. After the impact, the driver goes back to its initial position and hits the high position end stops causing nail gun body radiation (Fig. 12e). Finally, the last event corresponds to the noise escaping from the opening where the motor and flywheel are located (Fig. 12f).

4 CONCLUSION

An approach has been proposed for improved noise source identification on nail guns using a microphone array together with a source identification algorithm based on recent development in the generalized cross-correlation technique. In addition to pneumatic nail gun source identification that has previously been reported in the literature, two other nail gun types have been studied, a gas and an electric one. The fact that noise maps are associated with short time segments has allowed for a good time separation of the noise sources on these three nail gun types. All three nail guns have a source in common, the impact of the nail driver assembly against the rubber end stops and, to a lesser extent, the impact of the nail driver assembly against the up position end stops. On the pneumatic type, the proposed approach allowed the identification of a not previously identified source, the air trigger exhaust, in addition to the confirmation of the other already identified sources. On the electric nail gun, it has been possible to identify other noise sources such as the electrical motor and flywheel noise and to show that they are secondary sources at a much lower level, which explains that this kind of nail gun was found to have the lowest overall A-weighted sound power level in the standardized test. The pneumatic nail gun is ranked second as its secondary source, the exhaust noise, contributes more significantly to the total level. The gas nail gun is ranked third as the gas explosion becomes the primary source.

Further improvements of this approach would be the use of a higher frequency sampling rate to be able to reduce further the length of the time segments. However, in the present state, this approach can already help nail gun manufacturers to understand the origin of noise on their products and implement noise reduction measures through redesign or the use of classical noise control techniques. The reduction of the common noise sources to all three nail guns relies on the minimization of the forces generated by the internal impacts between the driver assembly and the nail gun body. The use of an air exhaust muffler could improve the pneumatic and gas nail gun total noise. Finally, body noise radiation could be reduced by using acoustic materials.

5 ACKNOWLEDGMENTS

The authors would like to acknowledge IRSST for the financial support (No 0099-6580).

6 REFERENCES

1. J. Howard, C.M. Branche, and G. Scott Earnest, “The new ANSI nail gun standard: a lost opportunity for safety”, *American Journal of Industrial Medicine*, **60**, 147–151, (2017).
2. E. Shanks, “Noise emission from fastener driving tools”, in *Health and Safety Laboratory for the Health and Safety Executive*, (2008).
3. R. Heaton, S. Hewitt, and L. Yeomans, “Correlation between vibration emission and vibration during real use: Fastener driving tools”, in *Health and Safety Laboratory for the Health and Safety Executive*, (2007).
4. M.-A. Gaudreau, F. Laville, P. Marcotte, and J. Boutin, “Laboratory and field measurements of nail guns' noise emission”, *Canadian Acoustics*, **44**(3), (2016).
5. D.A. Hicks, K. Vu, and M.D. Rao, “Study and reduction of noise from a pneumatic nail gun”, *Proc. NOISE-CON, Proceedings of the National Conference on Noise Control Engineering*, Cleveland, Ohio, (2003).
6. Z. Nili Ahmadabadi, F. Laville, and R. Guilbault, “Time domain identification and ranking of noise sources in a pneumatic nail gun”, *Applied Acoustics*, **114**, 191–202, (2016).
7. V. Jayakumar, J. Kim, and E. Zechmann, “Identification of noise sources and design of noise reduction measures for a pneumatic nail gun”, *Noise Control Engr. J*, **63**(2), (2015).
8. T. Padois, P.-A. Gauthier, and A. Berry, “Inverse problem with beamforming regularization matrix applied to sound source localization in closed wind-tunnel using microphone array”, *Journal of Sound and Vibration*, **333**, 6858–6868, (2014).
9. T. Padois and A. Berry, “Orthogonal matching pursuit applied to the deconvolution approach for the mapping of acoustic sources inverse problem”, *J. Acoust. Soc. Am.*, **138**(6), 3678–3685, (2016).
10. N. Quaegebeur, T. Padois, P.-A. Gauthier, and P. Masson, “Enhancement of time-domain acoustic imaging based on generalized cross-correlation and spatial weighting”, *Mec. Sys. and Sig. Proc.*, **75**, 515–524, (2016).
11. J. Velasco, D. Pizarro, and J. Macias-Guarasa, “Source localization with acoustic sensor arrays using generative model based fitting with sparse constraints”, *Sensors*, **12**, 13781–13812, (2012).

12. C. Knapp and G.C. Carter, "The generalized correlation method for estimation of time delay", *Transactions on Acoustics, Speech and Signal Processing, IEEE*, **24**(4), 320–327, (1976).
13. T. Padois, O. Doutres, F. Sgard, and A. Berry, "On the use of geometric and harmonic means with the generalized cross-correlation in the time", *J. Acoust. Soc. Am.*, **140**(1), EL56–EL61, (2016).
14. T. Padois, "Acoustic source localization based on the generalized cross-correlation and the generalized mean with few microphones", *J. Acoust. Soc. Am.*, **143**(5), (2018).
15. T. Padois, F. Sgard, O. Doutres, and A. Berry, "Acoustic source localization using a polyhedral microphone array and an improved generalized cross-correlation technique", *Journal of Sound and Vibration*, **386**, 82–89, (2017).
16. C. Noel, V. Planeau, and D. Habault, "A new temporal method for the identification of source directions in a reverberant hall", *Journal of Sound and Vibration*, **296**(3), 518–538, (2006).
17. *Acoustics — Determination of sound power levels and sound energy levels of noise sources using sound pressure — Engineering methods for an essentially free field over a reflecting plane*, International Standard ISO 3744, (2010).
18. *Acoustics. Noise test code for fastener driving tools. Engineering method*, International Standard EN 12549, (2008).